DEVELOPMENT OF HYBRID TYPE SELF-BEARING MOTOR WITHOUT EXTRA BIAS PERMANENT MAGNETS

Hideki Kanebako
Dept. of Mechanical Eng., Ibaraki University, Hitachi, 316-8511, Japan
hideki.kanebako@sankyoseiki.co.jp

Yohji Okada
Dept. of Mechanical Eng., Ibaraki University, Hitachi, 316-8511, Japan
okada@mech.ibaraki.ac.jp

ABSTRACT
A segmented permanent magnet rotor is proposed to generate sinusoidal flux density for hybrid type self-bearing motor. It also provides bias flux for the hybrid type magnetic bearing without extra bias permanent magnet. Hence the construction of self-bearing motor is simpler and reliable. First, the concept of the proposed hybrid type self-bearing motor is introduced. Then the radial force is analyzed to be proportional to the average air gap flux density, even though the air gap flux includes some opposite pole parts. Finally, the experimental setup is made to confirm the capability of the proposed motor. It can run up to 12,000 [rpm] and record 0.15 N.m/A torque and 9.8 N/A radial levitation force constants. The levitation is very stable. The motor has high performance for practical application.

INTRODUCTION
Several types of self-bearing motor have been introduced which are the combination of rotary motor and magnetic bearing [1]. These motors can support the rotor without physical contact and give rotating torque to the rotor. This replaces the contact components and leads to an overall reduction of size. In the previous works, P plus 2 or P minus 2 algorithm has been proposed to realize combined motor-bearing function [2]. But, it requires two kinds of rotating magnetic flux for rotation and levitation force respectively. Hence the construction of the motor and the control system are complicated.

To overcome this difficulty, a hybrid active magnetic bearing type self-bearing motor is proposed [3],[4]. It is also intended for the rotor to have two functions of rotary motor and radial magnetic bearings. The hybrid type self-bearing motor uses DC magnetic flux to control radial force. The radial force and rotating torque is independent when the pole pair number is more than three [3],[4]. Hence the structure of self-bearing motor and its control system can be simplified. But, it still requires rotor permanent magnets for rotation and bias permanent magnets for hybrid AMB.

In this paper, a segmented permanent magnet rotor is proposed to generate sinusoidal form flux density distribution for motor torque and a bias flux for hybrid AMB without additional bias permanent magnets. Hence the construction of the hybrid type self-bearing motor is even simpler. First, the concept of proposed hybrid type self-bearing motor is introduced. Then it is shown that the radial force is proportional to the average air gap flux density distribution, even though the air gap flux density distribution includes some opposite pole segment. Finally, the experimental setup is made to confirm the capability of the proposed motor. The results show high capability of the proposed self-bearing motor.

THEORETICAL CONSIDERATION
Motor Structure
Figure 1 shows the schematic drawing of the previous hybrid type self-bearing motor, while Fig. 2 shows the schematic drawing of the proposed self-bearing motor.

The left side of Fig. 1(b) is the self-bearing motor, while the right side is the hybrid type magnetic bearing. Between them permanent magnets are installed which give the bias flux as shown by the solid line.

The front view indicates the construction of the self-bearing motor. The stator has two kinds of windings; one is for levitation control and another is for rotation. There are two levitation coils for x and y directions, both of them are two pole windings. They produce the control flux as shown by the dotted line in Fig. 1(a) and produce radial force. The rotation can be controlled by the same manner of conventional permanent magnet motor.

On the contrary, the left and right sides of Fig. 2(b) are both self-bearing motors. Four segmented permanent magnets of S pole are glued on the surface of the left side rotor, while four segmented permanent magnets of N pole are attached on the surface of the right side rotor. Therefore, magnetic circuit is established between two rotors as shown by the solid line in Fig. 2(b), and the

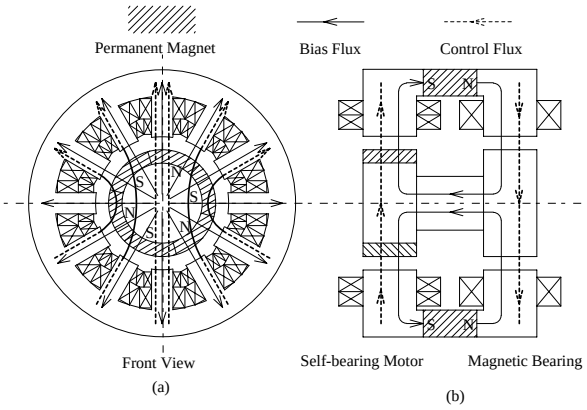

FIGURE 1: Schematic of hybrid type combined motor-bearing

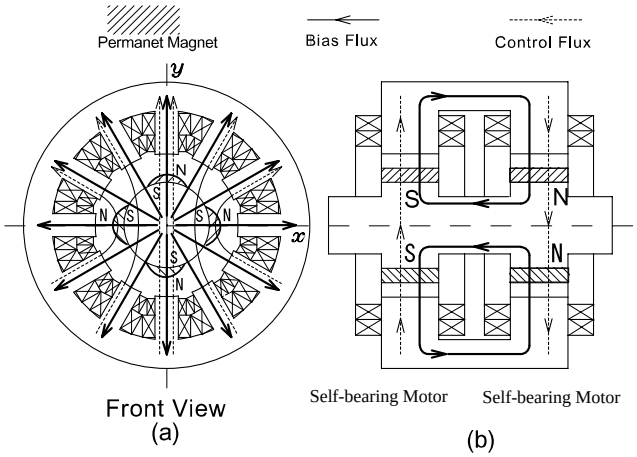

FIGURE 2: Schematic of proposed hybrid type combined motor-bearing

radiated bias flux is produced as shown by the solid line in Fig. 2(a) without extra bias permanent magnet.

Levitation Force

The motor coordinate system is determined as shown in Fig. 3. The flux distribution produced by rotor magnet B_r, the flux distribution produced by motoring coil B_{sm} and the radial force control flux B_{sb} are shown in Fig. 4. Because the proposed motor does not have bias permanent magnet, some opposite pole parts are appeared between the adjoining magnets on the rotor surface as shown in Fig. 5.

Authors have been theoretically derived that the independent control of levitation and rotation can be realized when the pole pair number is more than three [3],[4]. However, the influence of some opposite pole parts was not considered. Therefore, the influence of opposite pole parts is investigated.

The fluxies B_r,B_{sm},B_{sb} are expressed as followed.

$$B_r = B_0 + B_1 \cos(M\theta - \omega t) \quad (1)$$

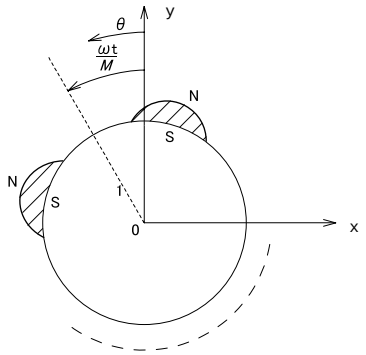

FIGURE 3: Coordinate system

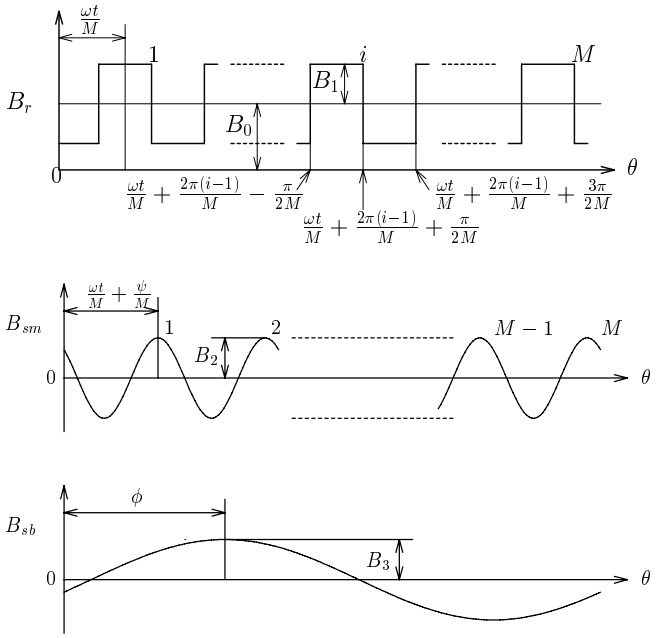

FIGURE 4: Flux density distributions

$$B_{sm} = B_2 \cos(M\theta - \omega t - \psi) \quad (2)$$

$$B_{sb} = B_3 \cos(\theta - \phi) \quad (3)$$

Then, the total flux distribution B_g in the air gap is given by

$$B_g = B_r + B_{sm} + B_{sb} \quad (4)$$

where

B_0	:	average bias flux density produced by rotor permanent magnet
B_1	:	peak flux value produced by rotor permanent magnet
B_2	:	peak flux value produced by motoring current
B_3	:	peak flux value produced by levitation current
θ	:	angular coordinate on the stator
ψ	:	phase of motoring flux

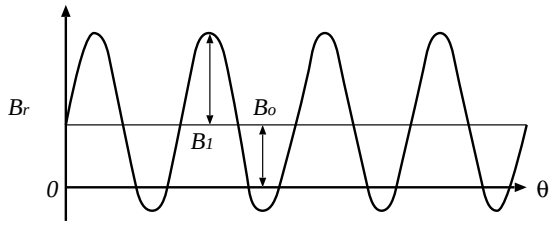

FIGURE 5: Flux density distribution of proposed motor

ϕ : phase of levitation flux
ω : angular velocity of the rotor
t : time
M : pole pair number $(= 1, 2, 3, \cdots)$
i : arbitrary integer

The radial force dF is calculated from the magnetic energy ΔW in an infinitesimal volume ΔV.

$$\Delta V = rlgd\theta \tag{5}$$

$$\Delta W = \frac{B_g^2}{2\mu_0}\Delta V = \frac{B_g^2}{2\mu_0} rlgd\theta \tag{6}$$

$$dF = \frac{\partial \Delta W}{\partial g} = \frac{B_g^2}{2\mu_0} rld\theta \tag{7}$$

where
r : radius of rotor
g : air gap between the rotor and the stator
l : length of rotor

Hence the x,y directional forces F_x,F_y are calculated by integrating the x and y components of dF over the entire gap.

$$F_x = \int_V dF\cos\theta = \int_0^{2\pi} \frac{B_g^2}{2\mu_0} rl\cos\theta d\theta \tag{8}$$

$$F_y = \int_V dF\sin\theta = \int_0^{2\pi} \frac{B_g^2}{2\mu_0} rl\sin\theta d\theta \tag{9}$$

From eqns.(8) and (9), the radial force can be controlled independently when $M \geq 3$, then we have

$$F_x = \frac{B_0 B_3 lr\pi}{\mu_0}\cos(\phi) \tag{10}$$

$$F_y = \frac{B_0 B_3 lr\pi}{\mu_0}\sin(\phi) \tag{11}$$

Hence F_x and F_y are independent of the rotor angle θ.

From eqns. (10) and (11), F_x and F_y are controlled by the levitation flux peak value B_3 and phase ϕ, and are not affected by the bias flux density distribution produced by rotor permanent magnet. Thus, the radial force is proportional to the average air gap flux density, even though the air gap flux includes some opposite pole parts.

EXPERIMENTAL TEST

Experimental Setup

Schematic of the experimental setup is shown in Fig. 6. There are two self-bearing motor A, B and thrust active magnetic bearing, hence five degrees of freedom can be controlled actively. For experimental simplicity, the thrust bearing is not operated. All four degrees can be controlled by the proposed motor.

TABLE 1: Self-bearing motor and AC servo motor specifications

	Self-bearing motor	AC servo motor
Structure	8 poles 12 slots	6 poles 9 slots
Stator inner diameter [mm]	ϕ33	ϕ33
Core thickness [mm]	30.8	39.2
Air gap (minimum) [mm]	0.8	0.3
Magnet thickness [mm]	2.5	3
Motor length [mm]	216	110
Coil diameter [mm]	ϕ0.4	ϕ0.8
Motor winding		
Turns	55	52
Resistance [Ω]	4.8	1.3
Inductance [mH]	8.8	1.3
Connection	Y(A,B parallel)	Y
Bearing winding		
Turns(maximum)	84	
Resistance [Ω]	7.3	
Inductance [mH]	4.8	

On the surface of left self-bearing motor A, four segmented neodymium magnets of S pole are glued with equal spacing, while four segmented magnets of N pole are glued on surface of the motor B rotor. Then, the bias magnetic circuit is produced through the shaft and the stator. The thickness of the segmented magnet is adjusted to generate a sinusoidal form flux density distribution.

The laminated sheet stator has 12 slots with 55 turns concentrated windings for motor coil. Each of them are connected 3 phase. The self-bearing motor A and B are connected to PWM power amplifier individually. The stator also has levitation windings for x and y directions. Each slot has concentrated windings and the number of turns are adjusted to generate a 2 pole sinusoidal form flux density distribution. The maximum turns of levitation windings are 84. The stator has inner diameter of 33[mm] and the length of 30.8[mm]. The air gap is 0.8[mm] excluding permanent magnets. An AC servo motor (typical output 450[W]) is used to compare with the proposed self-bearing motor performance. The specifications are listed in Table 1.

Schematic of the control system is shown in Fig. 7. The

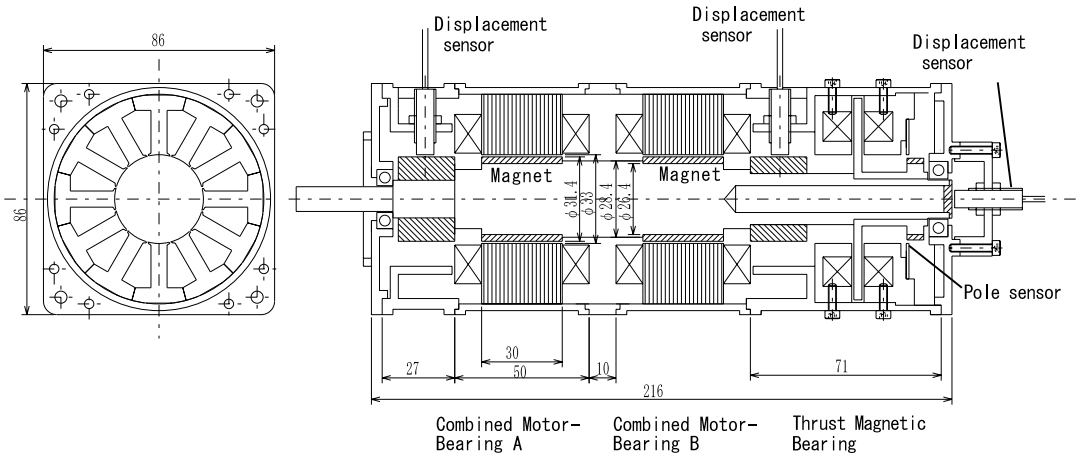

FIGURE 6: Schematic of Experimental Setup

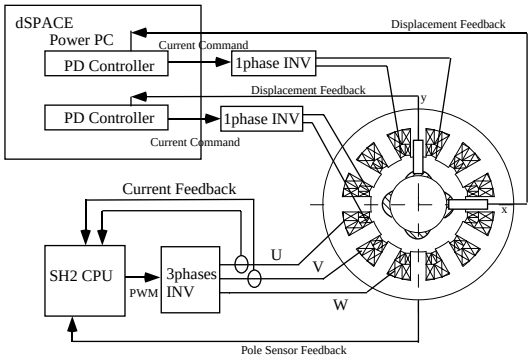

FIGURE 7: Control System

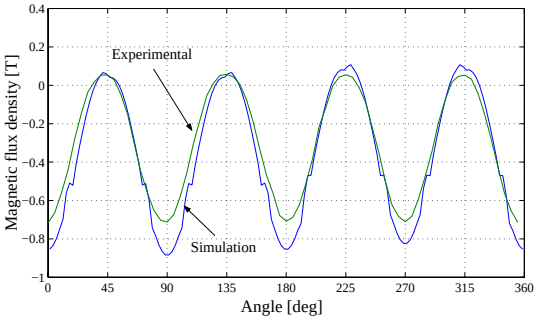

FIGURE 8: Flux Density of the Rotor

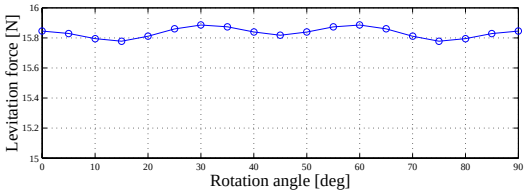

FIGURE 9: Levitation Force versus Rotating Angle

motor windings are driven by the standard three phases PWM inverter based on the pole sensor feedback. The bearing windings are driven by single phase PWM amplifier respectively. The single phase PWM amplifier has current feedback, hence the current command is applied to PWM amplifier from the levitation controller.

The levitation is controlled by a PowerPC board (dSPACE,DS1103). Radial displacements of x and y direction of the motor A and B are measured and put into the CPU via 16 bits A/D converters. Then the actuating signals are calculated using the standard PD controller for each direction.

Magnetic Flux and Levitation Force

To confirm the effect of opposite poles of air gap flux density described above, FEM simulation has been carried out. Figure 8 shows the flux density of the rotor. Both of experimental and simulation results have good sinusoidal form flux density distribution, and four segments of opposite pole is recognized. However, the experimental value is smaller than the simulation mainly due to magnetic saturation in the shaft. In this effect, the average bias flux density B_r and levitation force are smaller than the calculated values.

The levitation force is calculated by changing rotating angle with 1 [A] levitation current as shown in Fig. 9. The levitation force is 16 [N/A] and the levitation force ripple is only 0.1 [N]. This shows that the levitation force is constant and independent from rotor angle, even though the air gap flux density distribution includes some opposite poles.

TABLE 2: Control Parameters

Self-bearing motor	A	B
$K_p[A/mm]$	30.25	27.5
$K_d[A \cdot sec/mm]$	0.0605	0.0495

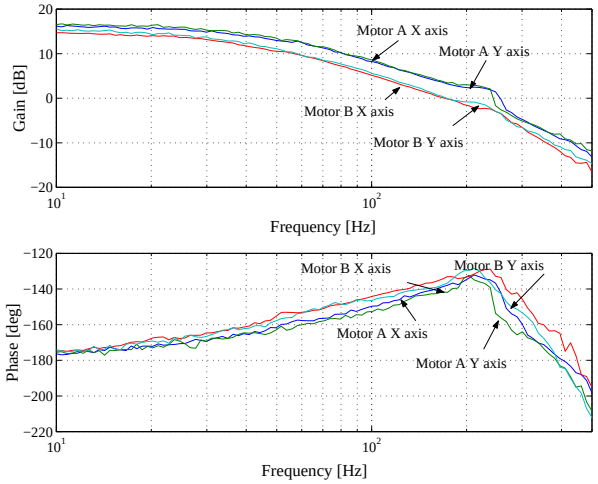

FIGURE 10: Frequency Responses

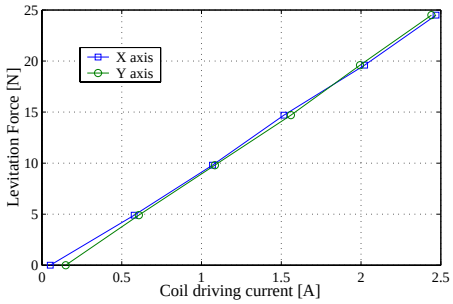

FIGURE 11: Levitation Force versus Current

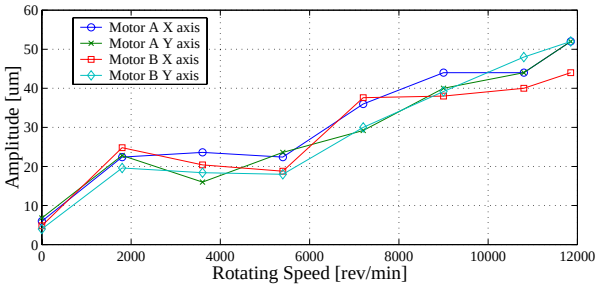

FIGURE 12: Vibration Amplitude versus Rotating Speed

RESULTS

To confirm the property of proposed motor, the levitated rotating tests are performed.

Levitation Control

The PD controller is used and determined experimentally as listed in Table 2. The frequency responses from feedback error to displacement sensor output is shown in Fig. 10. Stable controller with 250[Hz] band width, 45[deg] phase margin and 10[dB] gain margin is achieved for each axis.

The radial force is measured by changing the levitation current up to 2.5[A] as shown in Fig. 11. The levitation force 9.8[N/A] is smaller than the simulation results (16[N/A]) mainly due to the magnetic saturation of the bias magnetic circuit. However, they show very good linearity.

Rotating test

The no-load rotating test is carried out. The rotor can run up to 12,000[rpm] as shown in Fig.12. The amplitude increases over 6,000[rpm] mainly due to the vibration mode was changed from cylindrical mode to conical mode. The maximum rotating speed 12,000[rpm] is not due to the stability of levitation control, but due to the low voltage limit of the driver amplifier.

Next, loaded rotating test is carried out and the rotor vibration is measured by changing rotating direction within small period as shown in Fig. 13. Because the rotating direction was changed quickly, the motor current increased up to 5[A] and large torque was generated. However, both x and y directional vibrations are very small within 40 $[\mu m]$. The levitation and the rotation are controlled separately, hence there are no information link each other.

Motor Characteristics

The efficiency and output characteristics are measured by using a torque meter and a power meter which is shown in Fig. 14. Figure 15 shows the characteristics of the AC servo motor (typical output 450[W]) for comparison. Both motors was driven by the same amplifier with 55[V] of driving voltage. The rotor has to be connected to the torque meter, so that the levitation control is not applied and the rotor is supported by ball bearings for the self-bearing motor. Hence, the mechanical bearing power loss is lager than levitated condition.

The maximum efficiency of the self-bearing motor is 90 [%] and the maximum output is 100 [W], in comparison with 85 [%] and 120 [W] for the AC servo motor. The motor length of the self-bearing motor is twice of the AC servo motor. However the self-bearing motor is designed as an experimental setup and there are many dead spaces. Therefor, small size, high output and good efficiency self-bearing motor will be realized by applying optimum motor design.

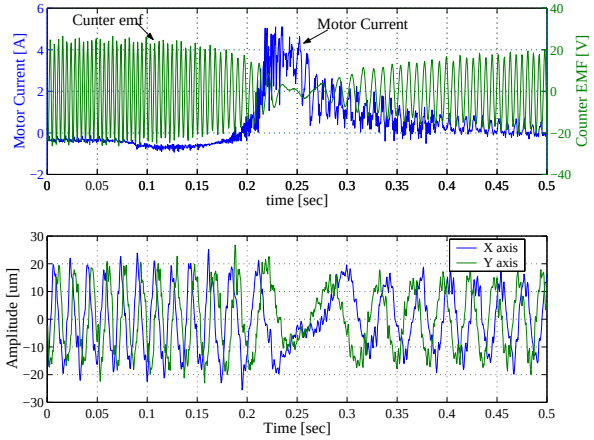

FIGURE 13: Acceleration Test

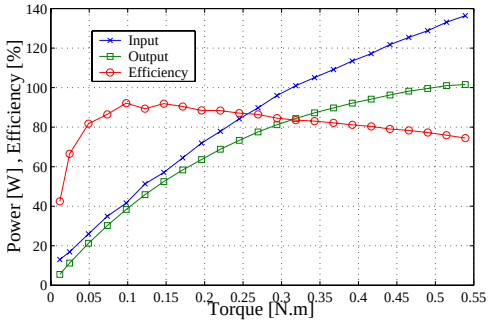

FIGURE 14: Self-bearing Motor Efficiency and Output Characteristics

Finally, the no-load power loss in comparison with the AC servo motor is measured as shown in Table 3. The power consumption of the self-bearing motor is 8[W] at 4,800[rpm] while the magnetic bearing power consumption is 21.9[W]. As a result, the no-load power loss of the self-bearing motor is 29.9[W] in comparison with 27.5[W] of the AC servo motor power loss at 4,470[rpm]. Since the self-bearing motor dose not have a speed depended mechanical power loss, the power loss of the self-bearing motor at even high rotating speed will be smaller than AC servo motor.

CONCLUDING REMARKS

A segmented permanent magnet rotor is proposed to generate sinusoidal flux density for motor torque and bias flux for levitation without using extra bias permanent magnet. The radial force is analyzed and confirmed experimentally to be proportional to the average air gap flux density, even though the air gap flux includes some opposite pole segments. The capability of the proposed motor is confirmed experimentally and compared with the AC servo motor. It can run up to 12,000 [rpm] and record 0.15 N.m/A torque and 9.8 N/A radial levitation force

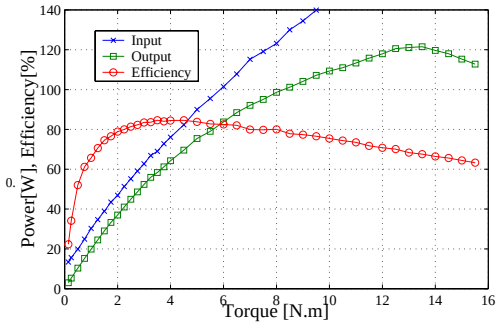

FIGURE 15: AC Motor Efficiency and Output Characteristics

TABLE 3: Self-bearing Motor and AC Servo Motor No-load Power Loss

	Self-bearing motor	AC servo motor
Rotating speed [rpm]	4,800	4,470
Power consumption [W]	8.0	27.5
Bearing power consumption [W]	21.9	
No-load power loss [W]	29.9	27.5

constants. The levitation is very stable. This motor has high performance for practical application. The comparison results with the AC servo motor show high capability of the proposed self-bearing motor.

References

[1] F. Matsumura, et. al., "State of the Art of Magnetic Bearings (Overview of Magnetic Bearing Research and Applications)",JSME Int. Journal, 40-4C (1997), pp. 553-560.

[2] Y. Okada, et. al., "Analysis and Comparison of PM Synchronous Motor and Induction Motor Type Magnetic Bearings",IEEE Trans. on Industry Applications, 31-5 (1995), pp. 1047-1052.

[3] Y. Okada, et. al., "Hybrid AMB Type Selfbearing Motor", Proc. of 6th Int. Symp. on Magnetc Bearings, Massachusetts, USA, August(1998), pp. 497-506.

[4] K. Shinohara, et. al., "Development of Hybrid Active Magnetic Bearing Type Combined Motor-Bearing", Trans. JSME, 66-642C (2000-2), pp. 503-508.(in Japanese)